© 2021. Published by The Company of Biologists Ltd | Journal of Experimental Biology (2021) 224, jeb239780. doi:10.1242/jeb.239780

RESEARCH ARTICLE

Dimorphic cocoons of the robin moth, *Hyalophora cecropia*, reflect the existence of two distinct architectural syndromes

Adam F. Parlin and Patrick A. Guerra*

ABSTRACT

The architectural design of animal structures forms part of an individual's extended phenotype that can be subjected to strong selection pressures. We examined cocoon architectural dimorphism in robin moths (*Hyalophora cecropia*), which construct multilayered silk-woven cocoons that possess either a 'baggy' or 'compact' morphology. These dimorphic cocoons reflect extended phenotypes that can enable survival during a critical developmental period (pupal stage to adult emergence), with cocoons occurring either sympatrically or as monomorphic groups across different climatic regions in North America. We hypothesized that cocoon dimorphism is related to the cocoon's role as a mediating barrier for moisture. We predicted that the macro- and micro-architectural differences between the cocoon morphs would be consistent with this function. We compared the cocoon morphs in terms of their orientation when spun under natural field conditions, examined how these orientations affected cocoon water absorption under simulated rain trials, and performed material surface tests to compare the hydrophobicity of cocoons. We found that compact cocoons had traits that increased water resistance, as they had significantly greater hydrophobicity than baggy cocoons, because they absorbed less water and released water vapor faster. In contrast, the increased water absorptiveness of baggy cocoons can allow for greater moisture retention, a function related to the prevention of desiccation. Our study suggests that cocoon dimorphism in robin moths reflects distinct architectural syndromes, in which cocoons are spun to optimize either water resistance or retention. These different functions are consistent with strategies that act to respond to uncertain external environmental conditions that an individual might encounter during development.

KEY WORDS: Animal architecture, Architectural syndrome, Dimorphism, Extended phenotype, Moisture regulation, Silk cocoon, Silk moths

INTRODUCTION

Extended phenotypes (Dawkins, 1982) represent traits external to the body of individuals that allow the interaction between genes and the environment, including animal architecture, parasite–host interactions or host manipulation (i.e. action at a distance). These interactions can lead to the selection and evolution of traits that are adaptive and therefore can increase the fitness of the individual (Dawkins, 2004; Bailey, 2012). Animal architectural structures, such as those made by insects (e.g. moth cocoons, beehives and termite mounds), arachnids (e.g. spider webs), birds (e.g. nests and mating displays) and mammals (e.g. beaver dams and mouse burrows) (Hansell, 2005) are examples of an individual's extended phenotype that can face selection pressure, thus changing in both form and function over time. Many architectural structures of insects facilitate homeostasis through biophysical interactions, such as the thermophysical benefits that can be provided by beehives, termite mounds and silk cocoons to the individuals residing inside (Guerra and Reppert, 2017; Schroeder et al., 2018). These structures can exhibit discrete or continuous phenotypic variation, and can evolve in part as a result of within-generational (i.e. individual plasticity) or trans-generational (e.g. effects of parental environment on their offspring) selection pressure from abiotic conditions and biotic interactions (Luquet and Tariel, 2016).

The silk-woven cocoons constructed by silk moth caterpillars in the genus *Hyalophora* (Lepidoptera; Saturniidae) are examples of animal architectural structures that can facilitate the protection of developing pupae against adverse environmental conditions (Danks, 2002, 2004; Guerra and Reppert, 2017; Guerra et al., 2020). Final instar larvae spin their own cocoon during the late summer, which protects the individual contained inside during a critical developmental period from the overwintering pupal stage to adult emergence in the following spring (Fedic et al., 2002; Danks, 2004; Horrocks et al., 2013). Individuals that do not survive abiotic environmental conditions and stressors during the overwintering period likely failed to maintain developmental homeostasis inside the cocoon and therefore do not contribute to the next generation. Although *Hyalophora* cocoons all possess the macro-architectural feature of two distinct layers, that of an outer and an inner envelope (Fig. 1A), there exists significant species-specific macro- and micro-architectural variation in cocoons within the genus (Guerra et al., 2020). The most striking of these is the intraspecific architectural difference between the dimorphic cocoons of the robin moth, *Hyalophora cecropia* (Waldbauer et al., 1982; Guerra and Reppert, 2017; Guerra et al., 2020). Robin moth caterpillars can spin either a large, loose and fluffy cocoon (baggy) or a much smaller and more tightly woven cocoon (compact) (Fig. 1). Here, cocoon dimorphism is manifested specifically as differences between the outer envelopes (Fig. 1B) and intermediate spaces of the two morphs, at both the macro-architectural (surface area and volume of the outer envelope; intermediate space volume) and micro-architectural (thickness and porosity of the outer envelopes) levels (Guerra and Reppert, 2017; Guerra et al., 2020).

Previous work has found that males and females construct similar baggy and compact cocoons (Waldbauer et al., 1982; Guerra and Reppert, 2017), and that there are no differences in adult size or condition as related to cocoon morphology (Guerra and Reppert, 2017). Moreover, the amount of silk used for the baggy or compact morphs is similar (Waldbauer et al., 1982; Guerra and Reppert, 2017), with the primary difference between the two cocoon morphs being how the silk is woven to construct cocoons with different

Department of Biological Sciences, University of Cincinnati, Rieveschl Hall, 318 College Drive, Cincinnati, OH 45221, USA.

*Author for correspondence (patrick.guerra@uc.edu)

P.A.G., 0000-0002-3647-6962

Received 21 October 2020; Accepted 2 April 2021

Journal of Experimental Biology (2021) 224, jeb239780. doi:10.1242/jeb.239780

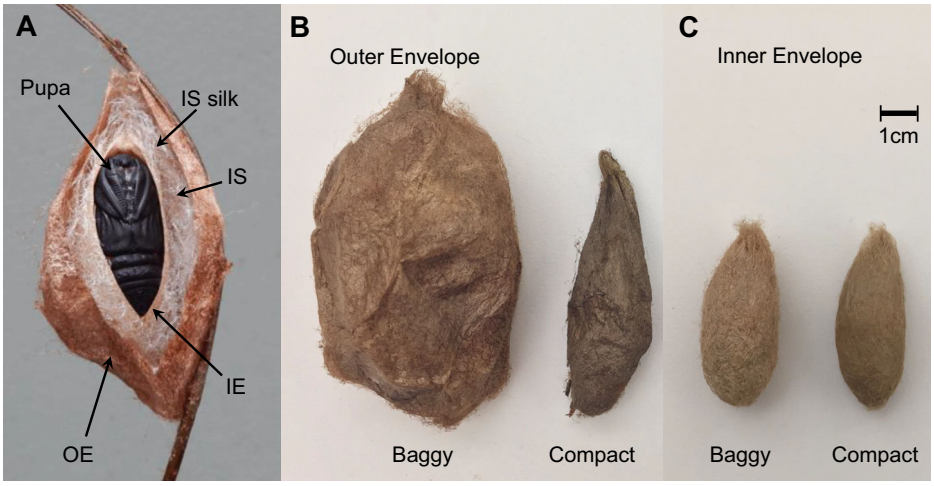

Fig. 1. Dimorphic cocoons of *Hyalophora cecropia*. (A) Labeled photograph of cocoon sections and pupa. OE, outer envelope; IS, intermediate space; IE, inner envelope. (B) Outer envelope of the baggy and compact morphs. (C) Inner envelope of the baggy and compact morphs. Scale bar refers to B and C. The photo in A was taken by S. M. Reppert and adapted from Guerra and Reppert (2017); photos in B and C were taken by P.A.G. and adapted from Guerra et al. (2020).

architectural structures and properties. The structure of the silk produced by *Hyalophora*, the material used for building cocoons, consists of parallel dual silk filaments (Sehadova et al., 2020) that are similar to those of the domesticated silk moth *Bombyx mori* in tensile properties but different in thickness (e.g. *Hyalophora* fibers are much finer) and amino acid composition (e.g. *Hyalophora* silk has more hydrophobic than hydrophilic amino acids) (Reddy and Yang, 2010). There is no difference in the type of silk used for construction between baggy and compact cocoons, and there is no difference in the type of silk used for making the outer and inner envelopes (Reddy and Yang, 2010; Guerra and Reppert, 2017). It has been observed that both cocoon morphs of robin moths can occur either sympatrically or as monomorphic groups across the extensive habitat range in North America (Guerra et al., 2020), which extends southwards from Southern Canada to Northern Florida, and westward from the Canadian Maritimes to the Rocky Mountains (Tuskes et al., 1996). There are also no differences in cocoon predation or parasitism between cocoon morphs (Waldbauer and Sternburg, 1967; Guerra and Reppert, 2017).

The existence of discrete, dimorphic cocoons in robin moths has been hypothesized to result from different selection pressures related to the varying habitat conditions in North America in which a cocoon can be spun (Collins, 2011; Guerra and Reppert, 2017; Guerra et al., 2020). For example, one proposed function of the different architectural cocoon morphs in robin moths is to control the level of moisture within the cocoon. Cocoons can facilitate increased internal humidity to prevent desiccation or function as a physical barrier to prevent excess water absorption to keep the individual dry at the pupal stage, especially when temperatures are colder in order to prevent lethal, inoculative freezing (Tagawa, 1996; Anderson and Brower, 1996; Danks, 2002, 2004; Guerra et al., 2020). While this species does accumulate glycerol during the pupal stage that can aid with supercooling (Wyatt and Meyer, 1959; Ziegler et al., 1979), the cocoon is vital to the survival of pupae during overwintering (Danks, 2002). Although previous work has shown that baggy cocoons can absorb more water than compact cocoons in laboratory submersion tests (Guerra and Reppert, 2017), it remains unknown whether the different cocoon morphs and their corresponding architectural features are specifically adapted to either promote or mitigate water absorption, thereby contributing to the evolution of architectural dimorphism in the robin moth. Each cocoon morph likely represents distinct architectural syndromes that include a suite of traits that make cocoons adapted for the uncertainty of overwintering environmental conditions. For instance, differing morphologies could be a result of a bet-hedging strategy for dealing with unpredictable environmental conditions (e.g. adaptive coin-flipping strategy), with specific advantageous traits related to moisture regulation (Guerra and Reppert, 2017; Guerra et al., 2020).

In our study, we used a comparative method to investigate how variation in the architectural features of dimorphic architectural structures within a species relates to potential adaptive functions. Specifically, we used a bottom-up approach to understand what properties of cocoons might explain and underlie the evolution of different architectural structures within a species, i.e. discrete variation in an extended phenotype between conspecifics, with a focus on studying the hydroproperties of these cocoons. Using robin moth cocoons as a model, we tested the hypothesis that intraspecific architectural dimorphism has evolved because the different cocoon morphs possess specific advantageous traits that can facilitate developmental homeostasis and survivorship in unpredictable environmental conditions. Specifically, we predicted that intraspecific architectural dimorphism in the cocoons of this species, manifested as distinct macro- and micro-architectural features between morphs, forms part of an individual's extended phenotype that is adapted for moisture regulation. To test our hypothesis, we first compared the macro-architecture of cocoons by assessing the orientations of cocoons that were constructed under natural field conditions. We then examined how these specific orientations might affect the level of water absorption in both baggy and compact cocoons, with and without the outer envelope present, in simulated rain trials. We compared the micro-architectural features of the cocoon morphs by examining their performance in material surface tests to determine whether or not they are hydrophilic or hydrophobic (i.e. water droplet contact, sliding and shedding angle tests; water droplet absorption tests; gas exchange trials). If the different cocoon morphs are in fact adapted for different moisture regulation functions, i.e. a hydrophilic or hydrophobic cocoon structure, then the two morphs should possess different and distinct macro- and micro-architectural features that can promote either one of these specific functions.

MATERIALS AND METHODS

Hyalophora cecropia cocoon collection

The *Hyalophora cecropia* (Linnaeus 1758) cocoons used in this study were all observed or collected outdoors and were spun by wild

Journal of Experimental Biology (2021) 224, jeb239780. doi:10.1242/jeb.239780

larvae under natural conditions (eastern Massachusetts – collected by S. M. Reppert or W. Greenwood; western New York state – collected by S. Morehouse). All cocoons were intact and free from damage (e.g. no holes due to predation or parasitoids). Adult *H. cecropia* that have eclosed within a cocoon will exit the cocoon via the valve at the top of the cocoon (Fig. 1; Tuskes et al., 1996). Unlike *Bombyx mori*, which secrete an enzyme (cocoonase) that damages the cocoon to enable them to exit it, because there is no exit valve, the cocoons of *H. cecropia* remain intact and are therefore testable in the subsequent experiments. Individuals from these cocoons successfully eclosed (larval and pupal exuviae were present) and exited the cocoon, indicating that the structure they constructed permitted diapause and survival during overwintering conditions. Experiments in our study used cocoons that were void of individuals, e.g. no live pupae, and therefore no animals were subjected to any form of experimentation.

Macro-architecture: cocoon orientation under natural conditions

We examined cocoons from pictures taken of them *in situ* at their outdoor spinning sites, to determine whether robin moth baggy and compact cocoons are each constructed with a specific orientation under natural conditions. We classified the orientation of cocoons found in northeastern USA based on the orientation of the long-axis of the cocoon relative to the ground, with the valve end of the cocoon considered the top of the cocoon and the long-axis extending from the valve to the bottom of the cocoon, and counted the number of observations (Fig. 2A). We classified cocoons as having been constructed with a vertical (perpendicular to ground), angled up (at any angle <90 deg and >0 deg), horizontal (parallel to ground) or angled down (below parallel) orientation based on the location of the valve relative to the ground (Fig. 2B–E). A single individual (P.A.G.) who was not involved with the search for cocoons scored the orientation of each cocoon.

We also conducted an online search for pictures of robin moth cocoons (keywords entered into the Google search engine: Saturniidae, *Hyalophora cecropia*, cocoon, baggy, compact, robin moth) found *in situ* outdoors at their spinning site, in order to supplement our examination of cocoon orientation (see Table S1 for the online sources of pictures). Three independent observers scored the orientation of each cocoon using the aforementioned criteria. Although the three independent observers were unable to come to a consensus on the morphology of the cocoons (i.e. baggy or compact) in pictures, they were able to reach a consensus on the orientation of the cocoon in a picture. Any cocoon images from our online search for which the observers could not reach a consensus on its orientation were omitted from analyses.

Macro-architecture: rain simulator trials

We used an indoor drip-type rain simulator (Fig. 3A; modified from Clarke and Walsh, 2007) to determine how the orientation and macro-architectural properties of the cocoon morphs affect cocoon water absorbance when exposed to simulated rain. Our rain simulator consisted of a commercially available rain simulator drip pan and stand (large expo model, Conservation Demonstrations, Salina, KS, USA) that had holes at the bottom to permit droplet formation. A moveable mesh droplet randomizer was gently and continuously swung back and forth within the path of the falling droplets during trials, to produce water droplets with a scattering size and distribution that resemble those of droplets found in natural rainfall (Clarke and Walsh, 2007; Fig. 3A).

We used baggy (n=10) and compact (n=10) cocoons collected in eastern Massachusetts (provided by W. Greenwood), and we removed any leaves or branches that were attached to the cocoons prior to trials. We then standardized the orientation of cocoons

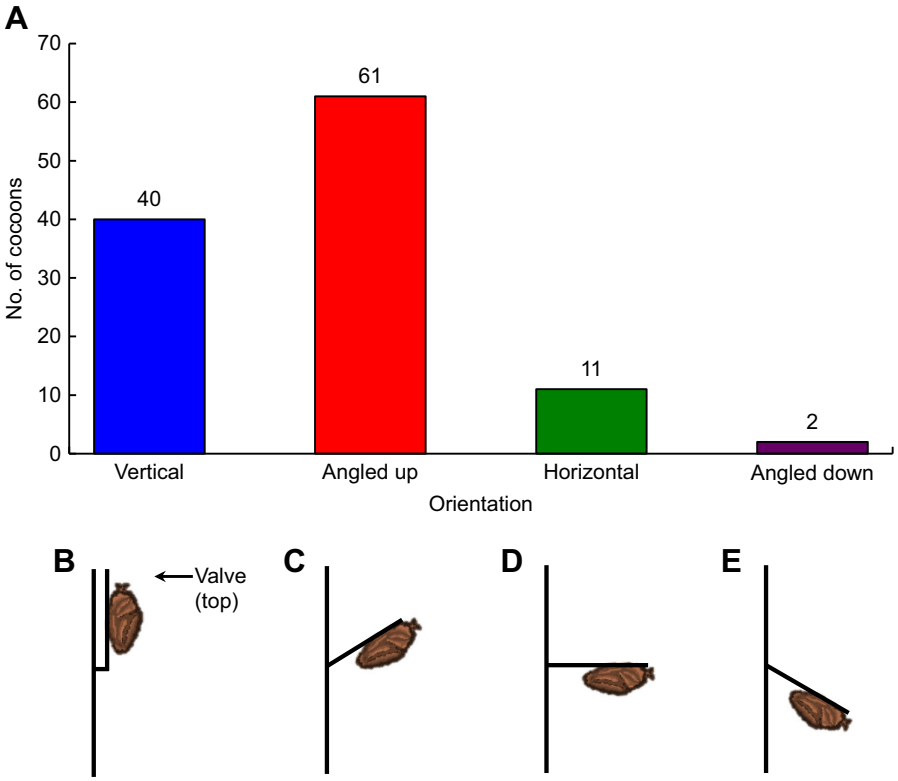

Fig. 2. Orientation of cocoons observed in the field and orientation definitions for online images. (A) The majority of cocoons found via our online search were spun with an angled up orientation. Numbers above bars indicate sample size. (B–E) Representations of the orientations of cocoons in images found via our online search. Each cocoon was classified as having (B) a vertical (perpendicular to ground), (C) an upward angle (up from ground), (D) a horizontal (parallel to ground) or (E) a downward angle (below parallel, oriented to the ground) construction orientation. The valve, indicated in B, represents the top of the cocoon, and is the same for B–E.

Journal of Experimental Biology (2021) 224, jeb239780. doi:10.1242/jeb.239780

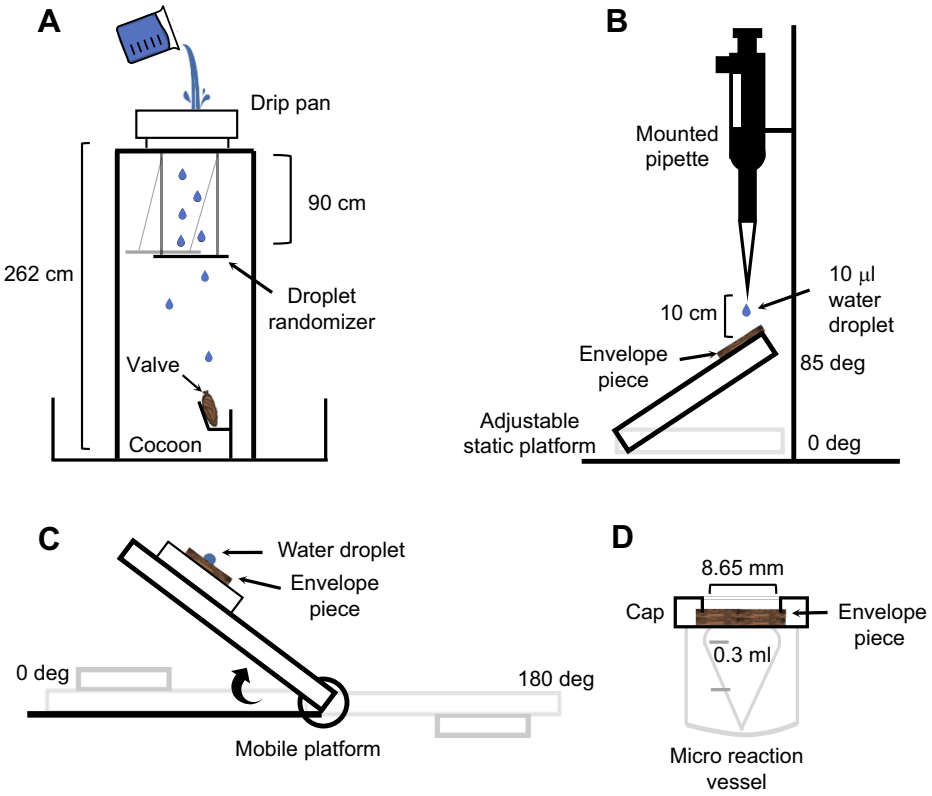

Fig. 3. Schematic diagrams of the different assays for our cocoon micro-architectural experiments. (A) Rain simulator. (B) Shedding angle apparatus with adjustable static platform. (C) Sliding angle apparatus with mobile platform. (D) Airtight micro reaction vessel for gas exchange.

across all trials, by gluing a wooden applicator stick parallel to the side of each cocoon. We first obtained the dry mass (cocoon and applicator stick) and then tested each of the baggy and compact cocoons as whole cocoons in rain simulator trials three separate times, once in each of three orientation positions, similar to those observed under natural conditions (Fig. 2B–D). The order of trials for each cocoon was randomized. For each trial, a cocoon was placed directly underneath the drip pan and droplet randomizer.

We tested each whole cocoon with a standardized 5 min treatment of simulated rainfall (10.51±4.63 mm, mean±s.d.; rainfall amount determined in pilot trials: n=18, 5 min of falling water droplets measured using a rain gauge). These trials are consistent with a 5 min rain event (10.67 mm of rain on 4 October 2011, 02:35 h EDT) measured with a rain gauge (Hyde Park, Boston, MA, USA; Boston Water and Sewer Commission, www.bwsc.org) from the respective geographical origins of our cocoons. At the end of each trial, we immediately weighed the combined mass of the whole cocoon, the applicator stick and any water that was absorbed by the cocoon to calculate the mass of water absorbed per trial. Cocoons were left to dry for a minimum of 24 h prior to subsequent trials. After the whole-cocoon trials, we removed the applicator stick from all cocoons and used a MakerBot Digitizer three-dimensional (3D) scanner (MakerBot Industries, New York, NY, USA) to obtain a 3D scan for each cocoon. We imported each 3D scan into the program netfabb Basic (version 5.2.0, Autodesk, Inc., Mill Valley, CA, USA) to obtain surface area (SA) and volume (V) measurements for each whole cocoon (outer envelope) (Guerra and Reppert, 2017). After scanning, we removed the outer envelopes from all cocoons and obtained a thickness (T) measurement for each outer envelope by measuring the thickness at the intersection point of the vertical and horizontal midline points (Guerra and Reppert, 2017) using digital calipers (iGaging Precision Instruments, San Clemente, CA, USA). We then removed the outer envelope and any silk found in the intermediate space of each cocoon, and repeated the rain simulator trials with these cocoons during which only the inner envelope was present. We used the same testing, weighing, scanning and thickness measurement protocols for the inner envelope cocoon trials.

The amount of water absorbed in simulated rain trials by the whole cocoon or the inner envelope by itself, for either baggy or compact cocoons, may be related to the SA, V or T of the different envelopes, three relevant cocoon envelope architectural traits that affect the biophysical properties of cocoons (Guerra and Reppert, 2017). While these traits are inherently different between the cocoon morphs, correcting for each specific trait can provide evidence for how each specific architectural trait contributes to water absorption. We therefore compared the cocoon morphs in terms of the amount of water that was absorbed by either the whole cocoon or the inner envelope alone, when corrected for SA [SA_c, water absorbed=absolute water absorbed/(V/T)], V [V_c, water absorbed=absolute water absorbed/(SA×T)] or T [T_c, water absorbed=absolute water absorbed/(V/SA)]. A significant difference in water absorption between the cocoon morphs when corrected by one of these factors indicates that the difference in the amount of water absorbed by cocoons was not due to that specific correction factor but instead to a different architectural parameter. Correcting for a factor controls for any influence of that architectural parameter on water absorption. Here, if baggy and compact cocoons are similar in water absorption after correction by a specific factor, this indicates that the architectural parameter of interest, V, T or SA, is a mediating factor of water absorption differences occurring between the cocoon morphs.

Micro-architecture: cocoon material surface tests

We tested whether the outer and inner envelope layers of baggy (n=10 per outer and inner envelope) and compact (n=10 per outer

and inner envelope) cocoons are either hydrophilic or hydrophobic, using three different metrics measured for a water droplet that was deposited on the envelope surface: (1) shedding angle, (2) sliding angle and (3) contact angle. For all tests, we used a representative section of the cocoon envelope that consisted of a 1 cm^2 envelope piece cut from the intersection of the vertical and horizontal midline point of the envelope using fine scissors (Guerra and Reppert, 2017). During each trial outlined below, an envelope piece was positioned over an open hole in a plastic platform and was held in place via adhesive tape along the outside edges of the silk piece. The envelope piece was oriented with the outside of the cocoon section, relative to the pupae housed in the cocoon, facing up for all tests. We allowed each envelope piece to fully dry (>24 h) between tests and experiments to avoid any influence of wetting in subsequent trials. We performed all trials at 21°C and at 22–25% relative humidity.

Shedding angle: static platform

We conducted shedding angle trials using a similar apparatus and protocol to those found in Zimmermann et al. (2009) (Fig. 3B) to determine the water-repelling ability of the cocoon. For each trial, we taped the envelope piece to the plastic platform that was affixed to a surface through which we could manipulate tilt (Fig. 3B). The angle for each trial was calibrated with a digital protractor (General Tools and Instruments, Secaucus, NJ, USA), and the test surface was held static during each trial. We applied a water droplet (10 µl) from a mounted pipette held in position above (10 cm) the envelope piece to fall and hit the envelope surface (Fig. 3B). For each envelope piece, we determined the shedding angle based on whether or not the droplet bounced or rolled upon contact. We started trials with the envelope piece positioned horizontally (0 deg) and progressively changed the angle of the platform by 5 deg for each trial, until we reached 85 deg of inclination. Immediately after each trial, we removed the envelope piece from the platform and inspected the underside of the envelope piece to determine whether water had gone through it during the trial. If the underside was wet, we scored the envelope piece as being saturated for that trial.

Sliding angle: mobile platform

We performed these trials using an apparatus modified from Ileleji and Zhou (2008) (Fig. 3C) and a protocol similar to Pierce et al. (2008) to determine the angle that a droplet will slide or roll at different droplet volumes (Miwa et al., 2000; Li et al., 2017). With the trial platform flat (0 deg), we deposited a water droplet on the envelope piece using a pipette. Once a droplet was deposited, we then changed the inclination of the surface and observed whether the water droplet slid or rolled off. Using a digital protractor to calibrate the movement of the platform, we changed the inclination angle of the platform in 10 deg increments and waited for 5 s prior to moving the platform to its next position to eliminate effects of kinetic energy. We moved the platform until it reached 180 deg from the starting position (i.e. upside down) and designated the angle at which the droplet slid or rolled off the envelope piece as the sliding angle. We performed four sets of trials, each at a different droplet volume (5, 15, 25, 35 µl). At the end of each trial, we immediately scored whether the envelope piece was saturated with water using the same method as in sliding angle trials.

Contact angle: static platform

We performed contact angle trials using an apparatus and protocol similar to those used in previous work that measures the contact angle of surfaces (e.g. Lamour et al., 2010; Rhim et al., 2006; Parlin et al., 2020), and measured the droplet height and diameter to determine water spreading or penetration relative to the cocoon (Yuan and Lee, 2013; Lee et al., 2016). The plastic platform was positioned horizontally (0 deg) for trials and we used a small leveler to verify its position (Bullseye Surface Level, Empire Level, Mukwonago, WI, USA). We deposited a standardized water droplet (5 µl) onto the envelope piece using a pipette. To avoid any effects of kinetic energy on the contact angle formed by the droplet, we used the sessile drop technique (Sun et al., 2017). We used a high-resolution digital camera (AVT Pike F421b, Allied Vision Technologies, Exton, PA, USA) equipped with a macro lens (Minolta 50 mm MD) to capture trials on video (Lamour et al., 2010). We used Fiji image analysis software to obtain sequential images for contact angle analysis (Schindelin et al., 2012).

A contact angle trial started when the droplet was on the surface and no longer in contact with the pipette (time=0 s). All trials lasted for 5 min. For each trial, we obtained three mean contact angles (mean of the contact angle of both sides of the droplet as seen in images) measurements: the initial contact angle (time=0 s); the dynamic contact angle (mean contact angle sampled every 5 s during the 5 min trial); and the final contact angle at the end of the trial. For the height and the width of the base of the droplet, we also made the same types of measurements, i.e. initial, dynamic and final height or width. At the end of a trial, we immediately inspected for saturation of the envelope piece using the method from our shedding and sliding angle trials.

Gas exchange

We compared the gas exchange rates of baggy and compact cocoons, for both their outer and inner envelopes, using two orientations. The orientations consisted of the envelope piece positioned in the micro reaction vessel to simulate either an inward-facing (water vapor absorption) or outward-facing (water vapor release) transfer of water vapor. We tested the gas exchange rates of the outer and inner envelopes of each cocoon morph as similarly done in previous work in an airtight vessel (Rhim et al., 2006; Horrocks et al., 2013; Parlin et al., 2020). Trials commenced by filling the micro reaction vessel with water (0.3 ml), and then measuring the starting mass of the apparatus (vessel, envelope piece, water) using an electric balance (Mettler-Toledo, model ME204E, Columbus, OH, USA; Fig. 3D). We then measured the change in mass of the apparatus, once every 24 h for a 96 h period, to determine the amount of water evaporated. We monitored the ambient temperature and humidity for the duration of these tests, in order to correct the water vapor transfer rate using equations outlined in Gennadios et al. (1994).

Statistical analyses

Prior to each set of analyses, we tested each data set to determine if it violated the assumptions of normality. We report the following effects sizes when applicable: partial eta squared (η_p^2), marginal r^2 and conditional r^2; Cohen's d (±95% CI) for parametric tests; effect size r (range) for non-parametric tests; Cohen's g for binomial tests. All subsequent analyses were performed in the program 'R' v3.4.3 (http://www.R-project.org/), except where otherwise indicated.

We compared the orientations of cocoons found under natural conditions (i.e. our pictures of cocoons from the Northeastern United States and cocoons from images found via our online search) with an exact multinomial test using the Xmulti package (https://CRAN.R-project.org/package=XNomial). This tested whether or not cocoons were constructed with a physical orientation at the spinning site that was biased towards any of the four orientations (i.e. Fig. 2B–E). If the overall exact multinomial test found that

cocoon orientation was not randomly distributed between the four orientation possibilities, we then conducted *post hoc* exact binomial tests to determine the probability of cocoons matching one of the four orientation categories (4 tests: Bonferroni-corrected α=0.0125).

We first compared the baggy and compact cocoons used in our rain simulator trials in terms of their SA, V and T using two-way ANOVA tests, in which we did separate analyses that compared the cocoon morphs in either their outer envelopes (a measure of whole-cocoon architectural metrics) or when they consisted of the inner envelope only. We also compared the volume of the intermediate spaces of the two cocoon morphs, in which the intermediate space volume was calculated by subtracting the volume of the inner envelope from the volume measured for the outer envelope (Guerra and Reppert, 2017). We then compared the performance of baggy and compact cocoons in rain simulator trials in two separate sets of statistical analyses. First, we compared the cocoon morphs when they were whole cocoons (outer envelope and intermediate silk present). Second, we compared the cocoon morphs when they consisted of only the inner envelope. For both sets of analyses, we performed a repeated measures mixed-model two-way ANOVA, with cocoon morph (baggy or compact) and orientation (vertical, angled or horizontal) as our two independent variables. In these analyses, we further determined whether SA_c, V_c or T_c influenced the water absorption of cocoons, by conducting six separate tests in which we corrected the water absorption values using one of these cocoon architectural traits.

For all of our material surface tests, we compared baggy and compact cocoons in two separate sets of analyses, one in which we compared their outer envelopes and another in which we compared the inner envelopes. We compared the shedding angle (mean angle), sliding angle (mean slide or rolling angle) and contact angle (mean, dynamic angle, droplet morphometrics) of both the outer and inner envelopes of baggy and compact cocoons. In shedding angle trials, we compared the mean shedding angle using unpaired *t*-tests. We compared the cocoon morphs in the propensity of the water droplet to slide or roll off the envelope piece at each droplet volume using Bonferroni-corrected Fisher's exact tests (α=0.0125, n=4 tests). In sliding angle trials, we compared the mean sliding angle at each droplet volume using unpaired *t*-tests. For contact angle trials, we used a mixed-model regressions (LMM) approach and analyzed these data using the *lme()*function ('nlme' R package, https://CRAN.R-project.org/package=nlme) in R (v3.6.4, http://www.R-project.org/). Cocoon ID was included as a random effect to account for repeated measures. We accounted for temporal autocorrelation using an autocorrelation structure, and we report the marginal and condition r^2 values for each model. Pairwise *post hoc* tests were conducted using the *glht()* function with Tukey contrasts ('multcomp' R package, https://cran.r-project.org/package=multcomp). We compared the cocoon morphs in terms of both their initial and final measurements of mean contact angle, droplet height and droplet base width using unpaired *t*-tests.

Within each of the three types of material surface tests, we also examined the saturation propensity of the deposited droplet as a measure of the cocoon morph's ability to absorb water. In shedding angle trials, we compared the number of tested angles in which saturation occurred between the cocoon morphs, for both outer and inner envelope pieces, using non-parametric Wilcoxon exact tests in JMP Pro (v14.0, SAS Institute Inc.). We compared the saturation propensity at each droplet volume tested in the sliding angle trials (5, 15, 25, 35 µl) for both the outer and inner envelopes of the cocoon morphs using Fisher's exact tests corrected for multiple comparisons (α=0.0125, n=4 tests). For saturation propensity in contact angle trials, we compared the outer and inner envelopes of the two cocoon morphs, using Fisher's exact test for each envelope comparison.

We also quantified the gas exchange rates of the outer and inner envelopes of both morphs, in order to compare their level of permeability as measured via water vapor transmission. We first corrected these water vapor permeability values (WVP_c) prior to analyzing them using unpaired *t*-tests. All unpaired *t*-tests were two-tailed tests.

RESULTS

Macro-architecture: propensity for cocoons to be spun at an angle in natural conditions

Overall, we found that cocoons are predominantly spun at an angle under natural conditions. This was the case both for the different cocoon morphs that were directly observed in the field and for cocoons assayed in pictures from the online search that we conducted.

From pictures of cocoons directly observed in the field, we examined 8 baggy cocoons (all from eastern Massachusetts) and 9 compact cocoons (2 from eastern Massachusetts and 7 from western New York). We found that the orientation of baggy cocoons was non-randomly distributed between the four orientation categories (exact test for multinomial, P=0.03; Fig. 2A). *Post hoc* exact binomial tests (Bonferroni-corrected α=0.0125) showed that the number of baggy cocoons that were spun at an upward angle was significantly greater than expected (n=6, P<0.01, Cohen's g=0.5). The number of cocoons spun vertical (n=1, P=0.69, Cohen's g=0.13), horizontal (n=1, P=0.69, Cohen's g=0.13) and at a downward angle (n=0, P=0.2139, Cohen's g=0.25) did not significantly deviate from the expected number of cocoons for each category. We also found that the orientation of compact cocoons was non-randomly distributed (exact test for multinomial, P=0.03806). *Post hoc* exact binomial tests showed that compact cocoons were spun at an upward angle with a frequency that was greater than expected (n=6, P<0.01, Cohen's g=0.42). Compact cocoons were spun at the expected frequency at all other orientations (vertical, n=2, P>0.99, Cohen's g=0.03; horizontal, n=1, P=0.47, Cohen's g=0.14; angled down, n=0, P=0.12, Cohen's g=0.25).

We found 118 unique online pictures of robin moth cocoons that were suitable for our analysis (Table S1). All three independent observers reached complete consensus on the orientation of the cocoon for 114 of these 118 pictures. We found that the orientation of these 114 cocoons was non-randomly distributed across the four orientation categories (exact test for multinomial, P<0.001). Using *post hoc* binomial tests (Bonferroni-corrected α=0.0125), we found that the number of cocoons spun with a vertical orientation (Fig. 2B) was consistent with the number of expected cocoons at this orientation (n=40, P=0.01688, Cohen's g=0.07). In contrast, there were significantly more cocoons spun at an upward angle than expected (n=61, P<0.001, Cohen's g=0.25), and there were significantly fewer cocoons than expected for horizontal (n=11, P<0.001, Cohen's g=0.28) and downward angle (n=2, P<0.001, Cohen's g=0.28) orientations.

Macro-architecture: parameters that influence water absorption during simulated rain

We found that the inherent architectural properties of both the outer and inner envelopes (i.e. surface area, volume and thickness parameters), and the intermediate space volume, differed between baggy and compact cocoon morphs. We found significant

Journal of Experimental Biology (2021) 224, jeb239780. doi:10.1242/jeb.239780

differences in surface area according to cocoon morph and envelope type (two-way ANOVA, interaction between cocoon morph and envelope type: $F_{1,36}$=118.1, P<0.001; morph η_p^2=0.78, envelope η_p^2=0.93, interaction η_p^2=0.76). The outer envelopes of baggy cocoons (SA=99.58±3.49 cm^2, n=10) had significantly greater surface area than the outer envelopes of compact cocoons (SA=49.54±2.68 cm^2, n=10), and both of these outer envelopes had greater surface area than the inner envelopes of both cocoon morphs (baggy SA=23.83±0.66 cm^2, n=10; compact SA=22.54 ±0.52 cm^2, n=10) (Tukey *post hoc* tests: P<0.05 for all comparisons). The inner envelopes of the two cocoon morphs had a similar surface area (Tukey *post hoc* test: P>0.05). Volume measurements also significantly differed according to cocoon morph and envelope type (two-way ANOVA, interaction between cocoon morph and envelope type: $F_{1,36}$=39.52, P<0.001; morph η_p^2=0.54, envelope η_p^2=0.78, interaction η_p^2=0.52). Baggy outer envelopes had the greatest volume (V=53.71±4.75 cm^3, n=10), followed by compact outer envelopes (V=21.04±1.8 cm^3, n=10), and both outer envelopes had greater volume than the inner envelopes of both cocoon morphs (baggy V=8.7±0.36 cm^3, n=10; compact V=8.2±0.30 cm^3, n=10) (Tukey *post hoc* tests: P<0.05 for all comparisons). The inner envelope volumes of both cocoon morphs were similar (Tukey *post hoc* test: P>0.05). Comparisons of the thickness of baggy and compact cocoons also showed that thickness significantly differed according to cocoon morph and envelope type (two-way ANOVA, interaction between cocoon morph and envelope type: $F_{1,36}$=12.06, P<0.01; morph η_p^2=0.48, envelope η_p^2=0.45, interaction η_p^2=0.25). Baggy outer envelopes were the thinnest (T=0.086±0.007 mm, n=10; Tukey *post hoc* tests for baggy outer envelopes versus each of the other groups, P<0.05). Compact outer envelopes (T=0.20±0.02 mm, n=10), baggy inner envelopes (T=0.20±0.01 mm, n=10) and compact inner envelopes (T=0.22±0.01 mm, n=10) had similar thickness (P>0.05 for all comparisons). Baggy cocoons also had an intermediate space volume (44.95±4.88 cm^3, n=10) that was greater than that of compact cocoons (12.89±1.85 cm^3, n=10) (unpaired Student's t-test t_{18}=6.13, P<0.001, Cohen's d=2.75±1.27).

Using our rainfall simulator, we found that water absorption can significantly differ between baggy and compact cocoons in different orientations (Fig. 4A). We found that, overall, the baggy and compact cocoons differed in the absolute amount of water absorbed, with baggy cocoons absorbing more water, but only when the outer envelope was present, i.e. for whole cocoons. The absolute amount of water absorbed by whole cocoons was significantly greater for baggy whole cocoons than for compact whole cocoons ($F_{1,45}$=81.54, P<0.001; morph η_p^2=0.63) (Fig. 4B), with both cocoon morphs absorbing the most water overall in the horizontal orientation ($F_{2,45}$=13.21, P<0.001; orientation η_p^2=0.35) (Fig. 4B). With the outer envelope and intermediate space silk removed, so cocoons only consisted of the inner envelope, baggy and compact cocoons had similar water absorption ($F_{1,45}$=2.61, P=0.11; morph η_p^2=0.05) (Fig. C). Only the orientation of cocoons affected the

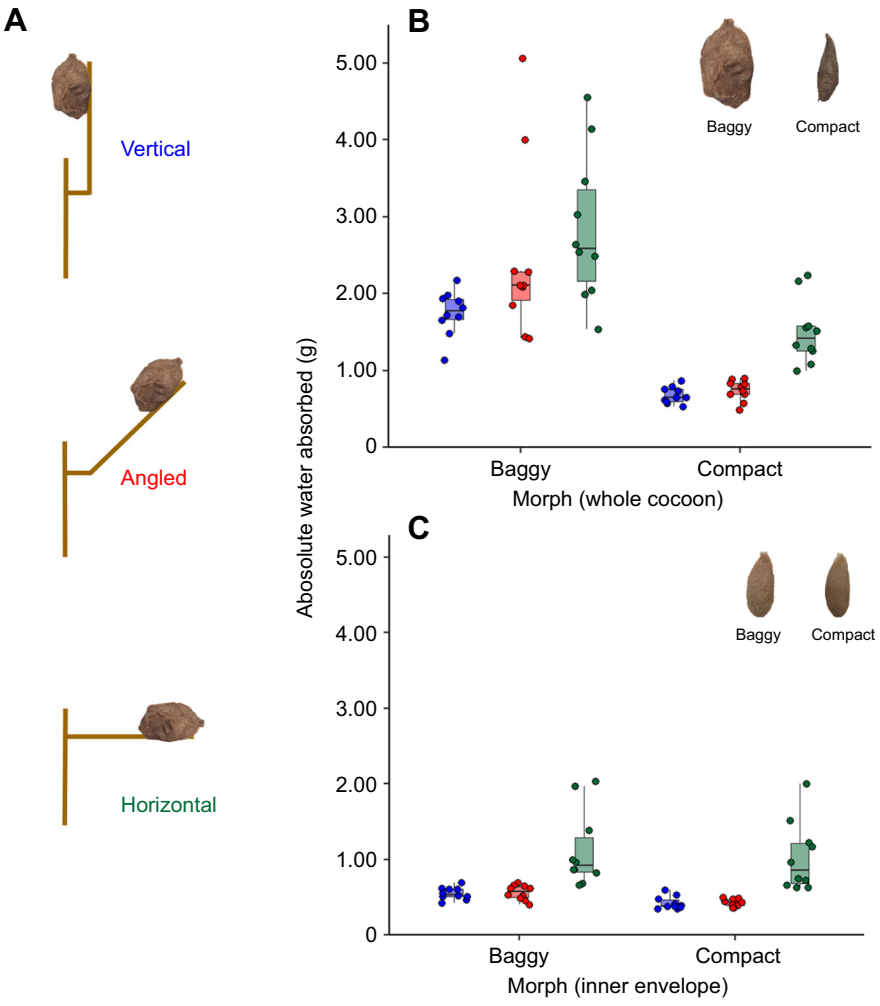

Fig. 4. Comparison of baggy (n=10) and compact (n=10) cocoon morphs in different orientations. (A) Vertical, angled and horizontal positions tested for water absorption during rainfall simulation trials. (B,C) Absolute amount of water absorbed for (B) whole cocoons and (C) inner envelopes only, during the simulated rainfall experiment, with measurements for vertical (blue), angled (red) and horizontal (green) cocoon trial orientations. Baggy whole cocoons absorbed more water than compact whole cocoons, and the amount absorbed increased as the orientation of cocoons went from vertical to horizontal.

Journal of Experimental Biology (2021) 224, jeb239780. doi:10.1242/jeb.239780

amount of water absorbed ($F_{2,45}$=28.18, P<0.001; orientation η_p^2=0.51), as the most water was absorbed when the inner envelopes were in the horizontal orientation (Fig. 4C).

When we corrected water absorption measurements for the SA, V or T of the cocoons, the baggy and compact cocoons differed in the amount of water absorbed as a result of the interplay between the cocoon architectural properties of the different envelope layers (V or T of the whole cocoon; SA, V or T of the inner envelopes alone) and the orientation of the constructed cocoon (vertical, angled or horizontal position) (Table 1). The difference observed between the whole cocoons of the cocoon morphs occurred at the three different orientations, but the difference between the cocoon morphs was most pronounced when cocoons were in the horizontal position (Fig. 4B). The horizontal position exposes more of the cocoon to the falling water in our rain simulator trials. Finally, the difference between whole baggy and whole compact cocoons, with whole baggy cocoons absorbing more water, was affected by the interplay between cocoon V and T (Table 1). Whole baggy cocoons can absorb more water than whole compact cocoons, as the outer envelope of baggy cocoons is thinner and has a larger intermediate space (Fig. 4B), allowing more water to penetrate into the cocoon and be contained within the cocoon during the same time frame.

The inner envelopes of baggy and compact cocoon morphs had similar water absorption, with both absorbing small amounts of water relative to when cocoons were whole (Fig. 4C). The amount of water absorbed by the inner envelopes of both cocoon morphs was affected by the interplay between V, T and SA (Table 1). Furthermore, the inner envelopes of both cocoon morphs absorbed the most water when tested in the horizontal position (Fig. 4C).

Micro-architecture: material surface tests show differences in hydrophobicity between cocoons

In shedding angle trials, we found that there were no differences in the mean shedding angle of baggy and compact cocoons when the droplet hit the surface of either the outer envelope (baggy 74.75±3.27 deg, n=10; compact 74.00±3.14 deg, n=10; unpaired t-test t_{18}=0.31, P=0.76, Cohen's d=0.14±0.88) or the inner envelope (baggy 53.75±1.76 deg, n=10; compact 53.75±1.22 deg, n=10; unpaired t-test t_{18}=−1.03, P=0.28, Cohen's d=0.49±0.89). There were significantly more tested angles at which saturation occurred during the shedding angle trials for the outer envelope of the baggy morph than for the outer envelope of the compact morph [baggy median=17, n=10; compact median=4, n=10; Wilcoxon exact test W=8.5, P<0.001; effect size r=0.72 (0.41–0.87)]. This indicates that the outer envelope of compact cocoons is better at repelling water than the outer envelope of baggy cocoons. There was no difference in saturation between the inner envelopes of baggy and compact morphs [baggy median=0, n=10; compact median=0, n=10; Wilcoxon exact test W=50.5, P=1; effect size r=0.01 (0.0098–0.5)], with the inner envelopes of the cocoon morphs similarly repelling water in trials.

In sliding angle trials, the water droplet remained on the outer envelope of both baggy (n=10) and compact (n=10) cocoon morphs, and did not penetrate and saturate through the envelope, for all the angles tested (0–180 deg). In comparisons between the inner envelopes of the cocoon morphs, there was no difference between the two morphs with respect to which angles the droplet slid off the inner envelope (Fisher's exact test, P>0.05 in all comparisons; n=10 for both baggy and compact outer envelopes), and the mean sliding angle was similar (baggy 53.32±6.33 deg, n=10; compact 51.47±5.21 deg, n=10; unpaired t-test t_{11}=0.21, P=0.83, Cohen's d=0.12±1.09). Compact cocoon inner envelopes had a lower saturation propensity than those of baggy cocoons, but only when a 5 µl water droplet was applied in trials (baggy 6/10 cocoons with saturation, compact 0/10 cocoons with saturation; Fisher's exact test, P=0.011 for 5 µl, P>0.05 for all other droplet volumes).

In outer envelope contact angle trials, the cocoon morphs had similar starting droplet morphometrics, as we found no difference between the cocoon morphs in starting contact angle (baggy 87.30±2.54 deg, n=10; compact 90.02±5.04 deg, n=10; unpaired t-test t_{18}=−0.46, P=0.65, Cohen's d=0.20±0.48), starting droplet height (baggy 0.14±0.002 mm, n=10; compact 0.15±0.006 mm, n=10; unpaired t-test t_{18}=−1.28, P=0.21, Cohen's d=0.57±0.89), and starting droplet diameter (baggy 0.24±0.01 mm, n=10; compact 0.25±0.01 mm, n=10; unpaired t-test t_{18}=−0.85, P=0.41, Cohen's d=0.38±0.88). The rate of change in droplet morphometrics differed between the outer envelopes of the cocoon morphs in two parameters (Fig. 5): the rate of change for contact angle (LMM χ_1^2=5.01, P<0.05; marginal r^2=0.14, conditional r^2=0.67) and for droplet height (LMM χ_1^2=5.1, P<0.05; marginal r^2=0.15, conditional r^2=0.72) was significantly faster for baggy outer envelopes than for compact outer envelopes. In contrast, the rate of change in droplet diameter was similar for the outer envelopes of the cocoon morphs (LMM χ_1^2=3.22, P=0.07; marginal r^2=0.09, conditional r^2=0.69) (Fig. 5). For final droplet morphometrics, we

Table 1. Two-way ANOVA comparison of water absorption for the whole cocoon and inner envelope for baggy and compact morphs, corrected for each relevant factor (SA_c, V_c, T_c), at three different orientations (vertical, angled, horizontal)

	SA_c				V_c				T_c			
Variable	d.f.	F	P	η_p^2	d.f.	F	P	η_p^2	d.f.	F	P	η_p^2
Whole cocoon												
Cocoon morph	1,45	61.28	<0.001	0.57	1,45	79.32	<0.001	0.62	1,45	61.28	<0.001	0.51
Orientation	2,45	15.82	<0.001	0.40	2,45	9.51	<0.01	0.29	2,45	15.82	<0.001	0.24
Cocoon×orientation	2,45	8.18	<0.001	0.26	2,45	1.22	**0.30**	0.05	2,45	1.44	**0.25**	0.05
Inner envelope												
Cocoon morph	1,45	0.27	**0.60**	0.01	1,45	6.72	<0.05	0.12	1,45	2.06	**0.15**	0.04
Orientation	2,45	21.75	<0.001	0.47	2,45	30.28	<0.001	0.54	2,45	27.65	<0.001	0.51
Cocoon×orientation	2,45	0.73	**0.49**	0.03	2,45	0.05	**0.95**	0.01	2,45	0.04	**0.96**	0.01

SA_c, corrected surface area; V_c, corrected volume; T_c, corrected thickness. Analysis included each variable (cocoon morph and orientation) as well as their interaction. For the whole cocoon, the most relevant parameters for water absorption were volume and thickness, two inherently different properties in each architectural structure that affected how much water was absorbed. For the inner envelope, all three parameters were relevant; however, water absorption was lowest in the vertical and angled positions and highest in the horizontal position. These results support the prior field observations where the horizontal position appeared less frequently. Bold indicates that the corrected trait had a significant effect on water absorption. See 'Macro-architecture: rain simulator trials' for more details.

Journal of Experimental Biology (2021) 224, jeb239780. doi:10.1242/jeb.239780

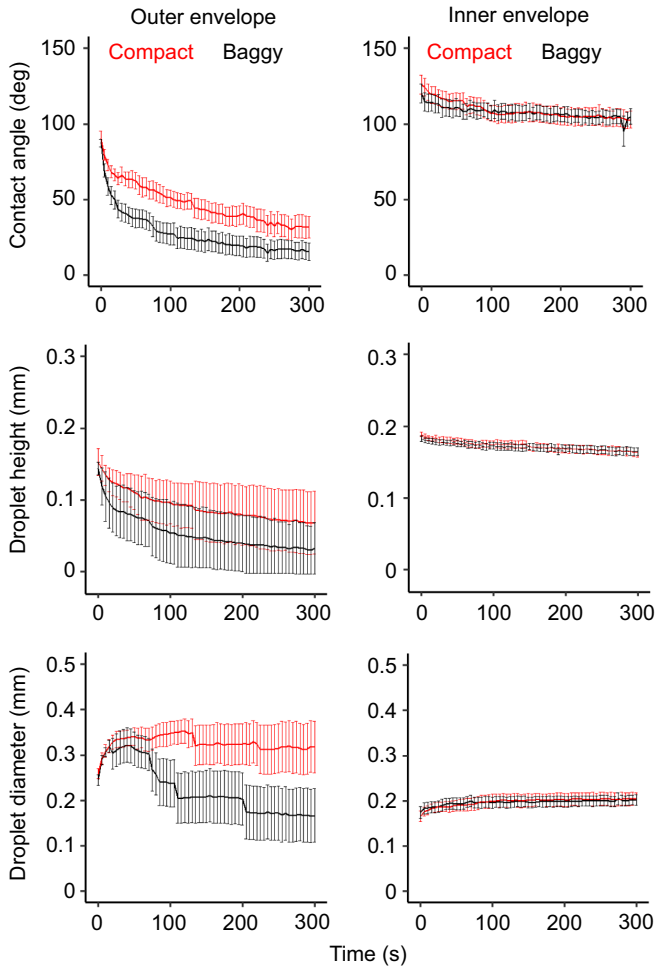

Fig. 5. Mean (±s.e.m.) droplet morphometrics for contact angle, height and diameter. Trials compared outer and inner envelopes of compact (red, n=10) and baggy (black, n=10) cocoon morphs over a 5 min period.

found no difference between the outer envelopes of the cocoon morphs in final contact angle (baggy 15.30±5.76 deg, n=10; compact 31.45±7.13 deg, n=10; unpaired t-test t_{18}=−1.67, P=0.11, Cohen's d=0.75±0.90), final droplet height (baggy 0.032±0.011 mm, n=10; compact 0.068±0.013 mm, n=10; unpaired t-test t_{18}=−1.91, P=0.07, Cohen's d=0.85±0.91) and final droplet diameter (baggy 0.17±0.059 mm, n=10; compact 0.32±0.056 mm, n=10; unpaired t-test t_{18}=−1.74, P=0.09, Cohen's d=0.78±0.90;).

In contact angle trials for the inner envelope, the cocoon morphs did not differ in any starting droplet morphometrics, as we found no difference in starting contact angle (baggy 87.30±2.54 deg, n=10; compact 90.02±5.04 deg, n=10; unpaired t-test t_{18}=−0.45, P=0.65, Cohen's d=0.27±0.88), starting droplet height (baggy 0.14±0.002 mm, n=10; compact 0.15±0.006 mm, n=10; unpaired t-test t_{18}=−1.28, P=0.21, Cohen's d=0.57±0.88) and starting droplet diameter (baggy 0.24±0.01 mm, n=10; compact 0.25±0.01 mm, n=10; unpaired t-test t_{18}=−0.85, P=0.41, Cohen's d=0.20±0.88). For the three dynamic droplet morphometrics, we found no significant difference between the inner envelopes of the cocoon morphs in their rate of change for dynamic contact angle (LMM χ^2_1=0.029, P=0.87; marginal r^2=0.001, conditional r^2=0.86), dynamic droplet height (LMM χ^2_1=0.058, P=0.0.81; marginal r^2=0.002, conditional r^2=0.84) and dynamic droplet diameter (LMM χ^2_1=0.004, P=0.95; marginal r^2=0.0001, conditional r^2=0.94) (Fig. 5). For final droplet morphometrics, we found no difference between the inner envelopes of the cocoon morphs in final contact angle (baggy 15.30±5.76 deg, n=10; compact 31.45±7.13 deg, n=10; unpaired t-test t_{18}=0.25, P=0.80, Cohen's d=0.11±0.88), final droplet height (baggy 0.032±0.011 mm, n=10; compact 0.068±0.013 mm, n=10; unpaired t-test t_{18}=0.17, P=0.86, Cohen's d=0.08±0.88) and final droplet diameter (baggy 0.17±0.059 mm, n=10; compact 0.32±0.056 mm, n=10; unpaired t-test t_{18}=−0.11, P=0.91, Cohen's d=0.05±0.88).

When we compared the envelopes of baggy and compact cocoons for saturation after contact angle trials, baggy outer envelopes absorbed more water than compact outer envelopes (baggy 10/10 with saturation, compact 4/10 with saturation; Fisher's exact test, P=0.011), but none of the inner envelopes of baggy and compact cocoons absorbed water (n=10 for both cocoon morphs). Overall, these results show that baggy outer envelopes let in more water than compact outer envelopes, but this occurs at the level of the outer envelope, as there was no difference in water absorption between the inner envelopes of the two cocoon morphs.

Our results also show that the outer envelope of compact cocoons had significantly higher corrected water vapor permeability (WVP_c) than the outer envelope of baggy cocoons, whether the cocoon piece was facing inwards (unpaired t-test t_{18}=−3.04, P=0.007, Cohen's d=1.37±1.0; Table 2) or outwards (unpaired t-test t_{18}=4.50, P=0.0002, Cohen's d=2.01±1.0; Table 2). This demonstrates that the outer envelope of compact cocoons permits faster water vapor transfer than that of baggy cocoons. We did not find a difference in the WVP_c of inner envelopes between baggy and compact cocoons, for either the outwards (unpaired t-test t_{18}=0.43, P=0.67, Cohen's d=0.19±0.88; Table 2) or the inwards (unpaired t-test t_{18}=0.25, P=0.80, Cohen's d=0.11±0.88; Table 2) orientation. These similar WVP_c values show that the inner envelope of the two cocoon morphs is comparable to the outer envelope of the compact cocoon, with faster water vapor transfer than the outer envelope of the baggy cocoon.

DISCUSSION

Distinct architectural syndromes

Consistent with our predictions, we found that the architecturally dimorphic baggy and compact cocoon morphs constructed by robin moths each possess a distinct suite of macro- and micro-architectural features. As extended phenotypes, the construction of two distinct cocoon morphs in robin moths, manifested at the level of the outer envelope and intermediate space volume (Fig. 1A), is consistent with the co-existence of two intraspecific architectural syndromes, with one potential architectural adaptation for making a structure that is hydrophilic (baggy cocoons) and the other for a

Table 2. Corrected water vapor permeability for outer and inner envelopes for the baggy and compact morphs

Orientation	Baggy cocoon WVP_c	Compact cocoon WVP_c
OE–Out	1.48±0.12^b	3.02±0.29^a
IE–Out	3.39±0.38^a	3.17±0.31^a
OE–In	1.40±0.13^b	2.76±0.40^a
IE–In	3.65±0.29^a	3.55±0.26^a

WVP_c, water vapor permeability (ng m^{-1} s^{-1} Pa^{-1}), as defined by Gennadios et al. (1994); OE, outer envelope (n=10); IE, inner envelope (n=10). 'Out' and 'In' indicate that the outside or inside, respectively, of the envelope piece was facing up in the micro reaction vessel apparatus during trials. Data are means±s.e.m. Significant differences from within-orientation comparisons of cocoon morph are indicated by different superscript letters (unpaired t-test; P<0.05).

structure that is hydrophobic (compact cocoons). Baggy cocoons are constructed to possess a physical orientation (angled: this study), outer envelope macro-architecture (thin membrane with a large volume: Guerra and Reppert, 2017; this study) and micro-architecture (porous membrane: Guerra and Reppert, 2017; hydrophilic properties: this study), and intermediate space architecture (a larger volume to hold more water: Guerra and Reppert, 2017; this study) that taken together facilitate enhanced water absorption and moisture retention by the baggy cocoon as a whole. In contrast, compact cocoons are spun with architectural features that promote water resistance, such as outer envelopes that are thick (Guerra and Reppert, 2017; this study), less porous (Guerra and Reppert, 2017) and possess hydrophobic surface properties (this study), as well as smaller intermediate spaces that can hold less water (Guerra and Reppert, 2017; this study). While the thicker outer envelope of compact cocoons is structurally less porous than the thinner outer envelope of baggy cocoons (Guerra and Reppert, 2017), when normalized for thickness the outer envelopes of compact cocoons released water vapor (via gas exchange) faster than the outer envelopes of baggy cocoons, and in a similar manner when compared with the inner envelopes of both cocoon morphs. The inner envelopes of both baggy and compact cocoons are structurally the same (Guerra and Reppert, 2017) and are functionally similar with respect to their hydroproperties (this study). It is important to note that males and females construct similar baggy and compact cocoons (at the level of both the outer and inner envelopes), the same amount and type of silk is used to construct cocoons whether baggy or compact, and that adult size and condition are independent of cocoon morphology (Waldbauer et al., 1982; Guerra and Reppert, 2017). Therefore, the weave of the silk itself in each cocoon morph likely facilitates the absorption of water (baggy) or water vapor release (compact) as the outer envelope of the baggy morph is significantly thinner and more porous than that of the compact morph, which highlights the primary difference between the cocoon morphs being associated with architectural structure and properties as shown in previous work (Guerra and Reppert, 2017).

These distinct architectural syndromes in robin moths are similar to the different syndromes that have evolved in other species, such as the dispersal and migratory syndromes seen across many diverse taxa including other insect species, birds, reptiles and mammals (Dingle, 2014). For instance, dispersers and migrants possess morphological structures, physiological processes, neural mechanisms and other correlated traits that facilitate efficient movement, such as to new resources or seasonally appropriate habitats. In contrast, resident, sedentary and non-migratory individuals can possess a contrasting suite of traits that allow individuals to better survive or be better competitors at the localities that they are found in and remain. The distinct architectural syndromes in the robin moth might have evolved in a similar manner, as each can convey certain advantages that the other syndrome does not provide, depending on the environmental context that the cocoon is found in (see below).

The role of architectural syndromes in environmental bet hedging

Diversifying extended phenotypes as part of an environmental bet-hedging strategy aids species by permitting survival in uncertain environments. Previous studies on *H. cecropia* have focused on the role of adult emergence throughout its native range in the northern and southern regions of North America (Sternburg and Waldbauer, 1969; Tuskes et al., 1996), specifically noting a potential genetic basis for a temporal pattern of bimodal emergence (i.e. early and late groups; Sternburg and Waldbauer, 1969). Here, a 'split the risks' strategy is suggested whereby early groups are favored in years with a mild spring followed by a summer of drought, and late groups would avoid losses due to cold and spring weather (Willis et al., 1974; Tuskes et al., 1996). However, there are no differences in emergence time, in terms of the time of year or the time of day, according to cocoon morph (Guerra and Reppert, 2017).

Given that cocoons can function as a protective structure for developing silk moths (Danks, 2002, 2004), why do discrete architectural morphologies with their corresponding different biophysical traits exist as extended phenotypes in the robin moth? Why is one cocoon type significantly more hydrophobic than the other in this species? The construction of baggy and compact cocoons has recently been suggested to be part of a diversified bet-hedging strategy that has evolved in response to environmental uncertainty (i.e. adaptive coin flipping; Guerra and Reppert, 2017; Guerra et al., 2020). The occurrence of hydrophilic and hydrophobic architectural syndromes in robin moths is consistent with a bet-hedging strategy related to moisture regulation as individuals of this species are found throughout North America and can experience either freezing (<0°C) or moderate (>5°C) overwintering conditions (Guerra et al., 2020). Here, individuals spin either one of the cocoon morphs as a hedge against stochastic environmental conditions that can be exacerbated by a lack or excess of moisture at the location of the cocoon during the pre-overwintering phase and during the subsequent spring. For example, baggy cocoon architecture may be advantageous in areas with drier conditions while compact cocoon architecture can protect the individual from environmental stress related to oversaturation with water. Anecdotal reports of robin moth cocoons possessing only compact morphology in the more northern and colder regions of the habitat range, and the co-occurrence of baggy cocoons with compact cocoons further south in the habitat range, are consistent with this bet-hedging strategy (Guerra et al., 2020). It is possible, however, that neither cocoon morph conveys a selective advantage to individuals within the cocoons despite differences in biophysical properties between the two types, and cocoon dimorphism remains in this species as it is a neutral trait with little to no selective disadvantage across the different habitat conditions in the robin moth range, or because cocoon dimorphism in *Hyalophora* is the ancestral state (Guerra et al., 2020). Future field observations are now needed to examine the proportion of baggy and compact cocoons throughout the robin moth's extensive and varied habitat and climatic regions in North America to test this hypothesis. Moreover, as we found significant differences in the biophysical properties (hydroproperties) of the different cocoon morphs that can be adaptive, our results have set the stage for future work to compare the overwintering success, pupal survival and hydroregulation, and the emergence phenology of individuals that are in either baggy or compact cocoons, to better understand the selective advantages that each cocoon architectural syndrome might convey to individuals under natural conditions.

Evolution of conspecific architectural syndromes

Intraspecific morphological dimorphism can evolve to either occur sequentially (e.g. seasonal or phase dimorphism) or simultaneously (e.g. dimorphism related to sex, caste or alternative strategies) in species. As an example of the former, in monarch butterflies, resident summer butterflies that are non-migratory are morphologically different from the following generation of fall monarchs that are morphologically adapted for long-distance migration (Reppert and de Roode, 2018). Morphologically

distinct individuals in this situation typically do not temporally and spatially co-exist. In contrast, morphologically different individuals can occur simultaneously in insect species that are wing or flight dimorphic, such as field crickets (Guerra, 2011). In this situation, individuals that are different morphologically can occur together as a result of life history trade-offs (e.g. increased reproductive output versus dispersal capability), or alternative life history and reproductive strategies. Architectural dimorphism in robin moth cocoons has evolved such that the two cocoon morphs can co-exist under the same habitat and environmental conditions (Guerra and Reppert, 2017; Guerra et al., 2020), suggesting that both morphs occur and are maintained in populations as each possesses a suite of advantages depending on the context, or at the very least they are both neutral phenotypes regardless of conditions. Because of contemporary environmental stressors such as climate change, which is accompanied by increased environmental stochasticity and a greater probability, intensity and duration of extreme weather events (e.g. drought, unseasonal cold conditions, intense autumn and winter storms), these architectural syndromes will likely face extreme selection pressure in the near future, and potentially undergo rapid evolution.

It remains unknown, however, what specific factors, whether intrinsic or extrinsic to the individual, mechanistically influence the construction of one cocoon morph over another. For example, previous work found that the sex of individuals, larval and adult size and condition, diet, habitat structure, environmental conditions and the topography of the cocoon-spinning site have little influence on which cocoon morph is spun by caterpillars in this species (Guerra and Reppert, 2017). Future studies that involve different parental crosses involving the two cocoon morphs, with individuals from different geographical and climatic regions in the habitat range of this species, are now needed to determine how genetics and environmental conditions might influence the expression of the two architectural syndromes.

Acknowledgements
We thank S. M. Reppert (eastern Massachusetts cocoons) and S. Morehouse (western New York cocoons) for providing us with pictures of cocoons from the field, and W. Greenwood for cocoons. We thank M. J. Alkema and J. Florman for the use of their equipment and for logistical support. We also thank the following for their assistance with trials and for logistical support: M. E. Albright, R. Clark, R. Jencen, M. J. Kendzel, S. Mahajan, J. Nathan and B. Thomas.

Competing interests
The authors declare no competing or financial interests.

Author contributions
Conceptualization: P.A.G.; Methodology: A.F.P., P.A.G.; Validation: A.F.P., P.A.G.; Formal analysis: A.F.P.; Investigation: A.F.P., P.A.G.; Resources: P.A.G.; Data curation: A.F.P., P.A.G.; Writing - original draft: A.F.P.; Writing - review & editing: A.F.P., P.A.G.; Visualization: A.F.P., P.A.G.; Supervision: P.A.G.; Project administration: A.F.P., P.A.G.

Funding
This research received no specific grant from any funding agency in the public, commercial or not-for-profit sectors.

References
Anderson, J. B. and Brower, L. P. (1996). Freeze-protection of overwintering monarch butterflies in Mexico: critical role of the forest as a blanket and an umbrella. *Ecol. Entomol.* **21**, 107-116. doi:10.1111/j.1365-2311.1996.tb01177.x

Bailey, N. W. (2012). Evolutionary models of extended phenotypes. *Trends Ecol. Evol.* **27**, 561-569. doi:10.1016/j.tree.2012.05.011

Clarke, M. A. and Walsh, R. P. D. (2007). A portable rainfall simulator for field assessment of splash and slopewash in remote locations. *Earth Surf. Process. Landf.* **32**, 2052-2069. doi:10.1002/esp.1526

Collins, M. M. (2011). Cocoons: reflections on their unappreciated natural history. *News Lepid Soc.* **53**, 39-43.

Danks, H. V. (2002). Modification of adverse conditions by insects. *Oikos* **99**, 10-24. doi:10.1034/j.1600-0706.2002.990102.x

Danks, H. V. (2004). The roles of insect cocoons in cold conditions. *Eur. J. Entomol.* **101**, 433-437. doi:10.14411/eje.2004.062

Dawkins, R. (1982). *The Extended Phenotype*. Oxford University Press.

Dawkins, R. (2004). Extended phenotype–but not too extended. A reply to Laland, Turner and Jablonka. *Biol. Philos.* **19**, 377-396. doi:10.1023/B:BIPH.0000036180.14904.96

Dingle, H. (2014). *Migration: The Biology of Life on the Move*. Oxford University Press.

Fedic, R., Zurovec, M. and Sehnal, F. (2002). The silk of Lepidoptera. *J. Insect Biotechnol. Sericology.* **71**, 1-15.

Gennadios, A., Weller, C. L. and Gooding, C. H. (1994). Measurement errors in water vapor permeability of highly permeable, hydrophilic edible films. *J. Food Eng.* **21**, 395-409. doi:10.1016/0260-8774(94)90062-0

Guerra, P. A. (2011). Evaluating the life-history trade-off between dispersal capability and reproduction in wing dimorphic insects: a meta-analysis. *Biol. Rev.* **86**, 813-835. doi:10.1111/j.1469-185X.2010.00172.x

Guerra, P. A. and Reppert, S. M. (2017). Dimorphic cocoons of the cecropia moth (*Hyalophora cecropia*): morphological, behavioral, and biophysical differences. *PLoS ONE* **12**, e0174023. doi:10.1371/journal.pone.0174023

Guerra, P. A., Lawson, L. P., Gatto, L. J., Albright, M. E. and Smith, S. J. (2020). Architectural evolution in cocoons spun by *Hyalophora* (Lepidoptera; Saturniidae) silk moth species. *Sci. Rep.* **10**, 5615. doi:10.1038/s41598-020-62547-1

Hansell, M. (2005). *Animal Architecture*. Oxford University Press.

Horrocks, N. P. C., Vollrath, F. and Dicko, C. (2013). The silkmoth cocoon as humidity trap and waterproof barrier. *Comp. Biochem. Physiol. A Mol. Integr. Physiol.* **164**, 645-652. doi:10.1016/j.cbpa.2013.01.023

Ileleji, K. E. and Zhou, B. (2008). The angle of repose of bulk corn stover particles. *Powder Technol.* **187**, 110-118. doi:10.1016/j.powtec.2008.01.029

Lamour, G., Hamraoui, A., Buvailo, A., Xing, Y., Keuleyan, S., Prakash, V., Eftekhari-Bafrooei, A. and Borguet, E. (2010). Contact angle measurements using a simplified experimental setup. *J. Chem. Educ.* **87**, 1403-1407. doi:10.1021/ed100468u

Lee, J. B., Radu, A. I., Vontobel, P., Derome, D. and Carmeliet, J. (2016). Absorption of impinging water droplet in porous stones. *J. Colloid Interface Sci.* **471**, 59-70. doi:10.1016/j.jcis.2016.03.002

Li, S., Huang, J., Chen, Z., Chen, G. and Lai, Y. (2017). A review on special wettability textiles: theoretical models, fabrication technologies and multifunctional applications. *J. Mater. Chem.* **5**, 31-55. doi:10.1039/C6TA07984A

Luquet, E. and Tariel, J. (2016). Offspring reaction norms shaped by parental environment: interaction between within-and trans-generational plasticity of inducible defenses. *BMC Evol. Biol.* **16**, 209. doi:10.1186/s12862-016-0795-9

Miwa, M., Nakajima, A., Fujishima, A., Hashimoto, K. and Watanabe, T. (2000). Effects of the surface roughness on sliding angles of water droplets on superhydrophobic surfaces. *Langmuir* **16**, 5754-5760. doi:10.1021/la991660o

Parlin, A. F., Stratton, S. M., Culley, T. M. and Guerra, P. A. (2020). A laboratory-based study examining the properties of silk fabric to evaluate its potential as a protective barrier for personal protective equipment and as a functional material for face coverings during the COVID-19 pandemic. *PLoS ONE* **15**, e0239531. doi:10.1371/journal.pone.0239531

Pierce, E., Carmona, F. J. and Amirfazli, A. (2008). Understanding of sliding and contact angle results in tilted plate experiments. *Colloid Surf. A Physicochem. Eng. As.* **323**, 73-82. doi:10.1016/j.colsurfa.2007.09.032

Reddy, N. and Yang, Y. (2010). Structure and properties of cocoons and silk fibers produced by *Hyalophora cecropia*. *J. Mater. Sci.* **45**, 4414-4421. doi:10.1007/s10853-010-4523-3

Reppert, S. M. and de Roode, J. C. (2018). Demystifying monarch butterfly migration. *Curr. Biol.* **28**, R1009-R1022. doi:10.1016/j.cub.2018.02.067

Rhim, J.-W., Lee, J.-H. and Hong, S.-I. (2006). Water resistance and mechanical properties of biopolymer (alginate and soy protein) coated paperboards. *LWT - Food Sci. Technol.* **39**, 806-813. doi:10.1016/j.lwt.2005.05.008

Schindelin, J., Arganda-Carreras, I., Frise, E., Kaynig, V., Longair, M., Pietzsch, T., Preibisch, S., Rueden, C., Saalfeld, S., Schmid, B. et al. (2012). Fiji: an open-source platform for biological-image analysis. *Nat. Methods* **9**, 676. doi:10.1038/nmeth.2019

Schroeder, T. B. H., Houghtaling, J., Wilts, B. D. and Mayer, M. (2018). It's not a bug, it's a feature: functional materials in insects. *Adv. Mater.* **30**, 1705322. doi:10.1002/adma.201705322

Sehadova, H., Guerra, P. A., Sauman, I. and Reppert, S. M. (2020). A re-evaluation of silk measurement by the cecropia caterpillar (*Hyalophora cecropia*) during cocoon construction reveals use of a silk odometer that is temporally regulated. *PLoS ONE* **15**, 0228453. doi:10.1371/journal.pone.0228453

Sternburg, J. G. and Waldbauer, G. P. (1969). Bimodal emergence of adult cecropia moths under natural conditions. *Ann. Entomol. Soc. Am.* **62**, 1422-1429. doi:10.1093/aesa/62.6.1422

Sun, M., Chen, Y., Zheng, Y., Zhen, M., Shu, C., Dai, Z., Liang, A. and Gorb, S. N. (2017). Wettability gradient on the elytra in the aquatic beetle *Cybister chinensis*

and its role in angular position of the beetle at water-air interface. *Acta Biomater.* **51**, 408-417. doi:10.1016/j.actbio.2017.01.022

Tagawa, J. (1996). Function of the cocoon of the parasitoid wasp, *Cotesia glomerata* L. (Hymenoptera: Braconidae): protection against desiccation. *Appl. Entomol. Zool.* **31**, 99-103. doi:10.1303/aez.31.99

Tuskes, P. M., Tuttle, J. P. and Collins, M. M. (1996). *The Wild Silk Moths of North America: A Natural History of the Saturniidae of the United States and Canada*. New York, USA: Cornell University Press.

Waldbauer, G. P. and Sternburg, J. G. (1967). Differential predation on cocoons of Hyalophora cecropia (Lepidoptera: Saturniidae) spun on shrubs and trees. *Ecology* **48**, 312-315. doi:10.2307/1933119

Waldbauer, G. P., Scarbrough, A. G. and Sternburg, J. G. (1982). The allocation of silk in the compact and baggy cocoons of Hyalophora cecropia. *Entomol. Exp. Appl.* **31**, 191-196. doi:10.1111/j.1570-7458.1982.tb03134.x

Willis, J. H., Waldbauer, G. P. and Sternburg, J. G. (1974). The initiation of development by the early and late emerging morphs of *Hyalophora cecropia*. *Entomol. Exp. Appl.* **17**, 219-222. doi:10.1111/j.1570-7458.1974.tb00339.x

Wyatt, G. R. and Meyer, W. L. (1959). The chemistry of insect hemolymph III. Glycerol. *J. Gen. Physiol.* **42**, 1005-1011. doi:10.1085/jgp.42.5.1005

Yuan, Y. and Lee, T. R. (2013). Contact angle and wetting properties. In *Springer Series in Surface Sciences*, vol. 51 (eds G. Bracco and B. Holst). Berlin, Heidelberg: Springer https://doi.org/10.1007/978-3-642-34243-1_1.

Ziegler, R., Ashida, M., Fallon, A. M., Wimer, L. T., Wyatt, S. S. and Wyatt, G. R. (1979). Regulation of glycogen phosphorylase in fat body of*Cecropia* silkmoth pupae. *J. Comp. Physiol.* **131**, 321-332. doi:10.1007/BF00688807

Zimmermann, J., Seeger, S. and Reifler, F. A. (2009). Water shedding angle: a new technique to evaluate the water-repellent properties of superhydrophobic surfaces. *Text. Res. J.* **79**, 1565-1570. doi:10.1177/0040517509105074